Available online **www.ijpras.com**

International Journal of Pharmaceutical Research & Allied Sciences, 2021, 10(4):131-141
https://doi.org/10.51847/Uh1ekmZM0d

Original Article

ISSN : 2277-3657
CODEN(USA) : IJPRPM

Neem Fruit Mucilage Impact on Acyclovir Release at Different Intervals : A Central Composite Design Screening

Gorantla Naresh Babu[1], Menaka Muthukarupan[2], Hindustan Abdul Ahad[3]*

[1]Department of Pharmaceutics, Balaji College of Pharmacy, Ananthapuramu-515001, Andhra Pradesh, India.
[2]Department of Pharmacy, Annamalai University, Annamalai Nagar-608002, Tamil Nadu, India.
[3]Department of Industrial Pharmacy, Raghavendra Institute of Pharmaceutical Education and Research (RIPER) - Autonomous, Ananthapuramu-515001, Andhra Pradesh, India.

***Email:** abdulhindustan@gmail.com*

ABSTRACT

The drive of this exploration is to look into the supportive mucoadhesive assets of neem (Azadirachta indica) fruit mucilage by incorporating it into mucoadhesive microspheres by taking Acyclovir (ACR) as a model drug. Nine interpretations of mucoadhesive microspheres were made with Methocel 934P and varying proportions of Neem fruit mucilage (NFM). A central composite design with design expert software to check the impact of independent variables (neem mucilage and methocel 934 P levels) on ACR release at 3h, 6h, and 10h as a response. As part of congeniality studies, the microspheres were examined for ACR content and its liberation. The research discovered that NFM can be used as an additive mucoadhesive polymer with Methocel 934 P and ACR can be systematically released in a controlled manner. The formulated microspheres were found to have good entrapment efficacy, mucoadhesion, drug contents, and other constraints assessed. NFM is capable of enhancing the mucoadhesion in combination with methocel 934 P and ACR can be retained in the stomach with its sustained release as mucoadhesive microspheres.

Key words: *Acyclovir, Factors, Microspheres, Mucoadhesive, Neem*

INTRODUCTION

Drug administrations are adopting unique attitudes to increase the gastric availability of drugs with patient consent. The gastro retentive microspheres, which are easy to prepare and administer, are of special importance among the various dosage forms [1].

Acyclovir (ACR) is a purine nucleoside analogue that is inevitable to tackle chickenpox, herpes simplex virus, and herpes zoster. ACR's oral bioavailability [1] has been appraised to 15-30%. ACR has a half-life of ~2 h. After oral administration, the ACR is well absorbed from the stomach [2, 3].

The properties of the polymer used in mucoadhesive systems greatly influence their effectiveness. The oral route is the preferred method of drug administration by many patients due to its convenience. For mucoadhesive drives, which are rare and expensive sometimes, many polymers have been tried. We are seeking a new polymer from nature that aids mucoadhesion. Using neem (*Azadirachta indica*) fruit mucilage (NFM), the authors intended to study the mucoadhesive microspheres. Studies have shown that NFM has antiviral properties [4]. Antiviral therapy may be aided by NFM. A steady-state systemic availability in expanded time is the objective of making mucoadhesive microspheres of ACR. As they are designed for ease, precision liberation systems are an effective solution for short-acting drugs and those that require continuous medicating [5].

Traditional research methods tend to focus on one variable at a time due to the ease of manipulating it. Statistically, each variable can be considered only once. Both factors will have an interrelationship, resulting in unreliable results. Design of Experiment (DOE) is understood as a treaty with a limited number of variables in multivariate analysis. In DOE, the objective is to screen for response and optimize. Every imitation of a Factorial design (FD) explores all conceivable amalgamations of the factors**.** In FD, the levels are called 'high' (+1) and 'low' (-1), and the input factors are called FD at two levels. In this study screening of mucoadhesive microspheres of ACR was studied to assess the impact of independent variables on response using design expert software [6, 7].
These authors plan to study the mucoadhesive properties of Neem fruit mucilage (NFM). Previous research has suggested NFM has antiviral properties. NFM may assist with antiviral therapy. NFM aims at achieving steady-state systemic availability for a protracted period. Precision liberation systems, designed for ease of use, are an effective way to release short-acting drugs.

MATERIALS AND METHODS

Materials
Acyclovir (ACR) was from Actavis Pharma, Bangalore. methocel 934P and dichloromethane were from Merck, Hyderabad.

Methods
Extraction of mucilage
As defined by Ahad *et al.,* 2010, [8] expressions were depleted. Following the washing of the neem fruits, they were soaked in water, boiled for an hour, and cooled. After the seeds were detached, partition was accomplished using petroleum ether (50%), ethyl acetate, and butanol. Using a multilayer muslin bag, the mucilage was mined to remove the marc. After being divided, parched in an oven at 40°C, poised, grounded, put through a # 80 sieve (Remi), and drained, the mucilage was stored in a desiccator at 30°C and 45% RH.

Cleaning of the mucilage
As defined by Ahad *et al.,* 2021, [9] after homogenization (Biologics 150VT) with 5% trichloroacetic acid, centrifugation (Remi R-303), neutralization with NaOH, and dialysis in the SURDIAL-X, the NFM was filtered. Lastly, ethanol (95%) was treated with acetone and diethyl ether until it was clean.

Experimental design
We used Design Expert Software (11.0.5.0, Stat-Ease Inc.) to create and judge quadratic response surfaces to optimize the NFM using 9 runs, and a central composite design (CCD). A quadratic model was created based on determining the boundarykey, and quadratic chattels of independent variables on dependent variables [10]:

$$Y= B_0+B_1 X_1+B_2X_2+B_{12}X_1X_2+B_1X_1^2 + B_2X_2^2 \quad (1)$$

The dependent variable is Y, the independent variables are X_1 and X_2, and the regression coefficients are B_0, B_1, and B_2. For NFM, the dependent variables/responses were drug release at 3h (Y_1), 6h (Y_2), and 10h (Y_3). A total of 9 experiments were used to design the variables and their levels used in the NFM optimization [11].
The ingredients in various NFM are listed in **Table 1**.

Table 1. Composition of the NFM

Components	Formulations								
	B-1	**B-2**	**B-3**	**B-4**	**B-5**	**B-6**	**B-7**	**B-8**	**B-9**
Acyclovir (mg)	200	200	200	200	200	200	200	200	200
Ethyl Cellulose (mg)	50	50	50	50	50	50	50	50	50
NFM (mg)	50	50	50	75	75	75	100	100	100
Methocel 934P (mg)	50	75	100	50	75	100	50	75	100
Dichloromethane (ml)	25	25	25	25	25	25	25	25	25
Span 80 (ml)	2	2	2	2	2	2	2	2	2
Glutaraldehyde (ml)	2	2	2	2	2	2	2	2	2
Liquid paraffin (ml)	250	250	250	250	250	250	250	250	250

Preparation of NFM

Dichloromethane and acetic acid were used to dissolve the methocel 934P, ACR, EC, and NFM. Using an IKA-R1385 three-bladed propeller stirrer (300 rpm), this mixture was continuously stirred into liquid paraffin (containing span 80). A concentration of 5 min per minute of 1ɑ3 glutaraldehyde was added dropwise (3h of stirring). After centrifugation and washing with petroleum ether, the Acyclovir-Neem mucoadhesive microspheres were removed from liquid paraffin. To remove residual 1ɑ3 glutaraldehyde from NFM, it was suspended in sodium bisulfite (5%) for 15 min later washed with distilled water. Vacuum desiccators were used to preserve the microspheres so formed [12].

Evaluation parameters

Identification of drug

ACR spectrum (FTIR) was compared with the reference spectrum to see if any functional groupings had changed.

Determination of melting point

The ACR melting point was evaluated by the open capillary method [13].

Drug Excipient compatibility studies

DSC

ACR and NFM were appropriated in a mini pan of DSC at 50–300°C in a 1:1 ratio (Venchal Scientific-412105–USA).

FTIR

By scanning on a 4000-400 cm^{-1} array, FTIR spectroscopy (Bruker) was used to examine the synergy between ACR and NFM.

Initial risk assessment

Quality by Design (QbD) is one of the characteristics of Quality Target Product Profile (QTPP) as described in ICH Q8 and Q9. The extraction of the unprejudiced at the beginning of the development of a product is similarly presumptive. A QTPP ensures that a product meets essential quality standards by utilizing product assets [14-16]. Based on previous explorations and literature judgments, we examined the QTPP and CQAs for the NFM.

Evaluation of physical properties

Particle size measurement

A stage micrometer scale was adopted to assess the microsphere's particle size by placing them on glass slides using an eyepiece micrometer and 100 particles were counted for each batch [17-19].

Production yield

The production yield was premeditated from the ratio of the mean weight of parched microspheres (W_1) recuperated from each of 3 trials to the total of the preliminary dry weight (W_2) [20, 21].

$$\%\text{Percentage Yield} = \frac{\text{Weight of the attained microspheres}}{\text{Total weight of drug and polymers}} \times 100 \quad (2)$$

Entrapment efficiency

100 mg of microspheres dispersed overnight in 0.1 M HCl and the mixture was filtered assessed at 254 nm spectrophotometrically (Elico Spectrophotometer, SL-174). Entrapment efficiency was determined by comparing the sum of ACR in the formulation with the amount initially added [22, 23].

$$\text{Entrapment efficacy} = \frac{\text{Practical drug yield}}{\text{Theoretical drug content}} \times 100 \quad (3)$$

Swelling measurement

The swelling of microspheres was conducted by keeping them in 0.1M HCl. After 3h, they were removed, centrifuged, and the weight gained was resolute by the difference in weight gained at time t (Xt) and the initial time (t = 0 [X0]) as deliberated from the following equation [15, 24].

$$\% \text{ SI} = \frac{\text{Xt} - \text{Xo}}{\text{Xo}} \times 100 \quad (4)$$

Where Xt-weight of the NFM after time t; Xo- Initial weight of the NFM

Mucoadhesion measurement study

Mucoadhesive time (MT) was judged with a piece of 5 cm of fresh sheep stomach that had been eviscerated and washed with isotonic saline within 60 min of the animal's death. Using a polyethylene plate that was immobile at a position of 40° relative to a straight line, we kept a precise microsphere weight on the mucosal surface. The tissue was applied at a rate of 5 ml/min with HCl (0.1M) warmed to 37±1°C. We measured how long it took the sheep to detach all of the microspheres from its mucosal surface [25-27].

$$\text{Force of adhesion (N)} = \frac{\text{Mucoadhesive strength (g)} \times 9.81}{1000} \quad (5)$$

In Vitro ACR release study

Microspheres were dispersed using the USP-II apparatus at a stirring rate of 50±5 rpm at a temperature of 37±0.5°C, using 900 ml of HCl (0.1N HCl) as a dissolution medium. A 5 ml sample at different breaks (replenished the volume of dissolution media at each break) and a spectrophotometric analysis were performed at 254nm on the samples. At 3h, 6h, and 10h, the amount of ACR released was recorded [28].

Statistical optimization

With Design-Expert, we estimated independent influences on retorts from contour plots (2D) and response surface plots (3D). Statistical validation of polynomial intentions was obtained by judging ANOVA eatables (software generated). The ANOVA endowment created a statistical model to determine model abundance and aptitude. An F value with a p-value of 0.05 [29].

RESULTS AND DISCUSSION

Identification of drug

When comparing the sample spectrum of ACR with the reference spectrum, there were no significant differences in the functional groups.

Determination of melting point

The standard melting point of ACR was in the array of 254.8±1.7℃

Compatibility studies

As a result of the DSC assessment, the pure ACR produced a sharp endothermic peak, representing the purity of the ACR. When combined with excipients that shifted left, this peak becomes broader. Observations of the DSC indicate there is no interaction between ACR and the excipients.

The ACR pure form spectrum shows FTIR bands for secondary amines, phenyl esters, and carboxylic groups. Blends (B-9) have peaks and stretches similar to pure drugs. Excipients in ACR did not obstruct peaks and stretches in its spectrum.

Physical properties

Particle size

For all formulations, particle size was determined using optical microscopy. The microspheres array ranges from 30.9±0.1 to 37.9±0.2 µm **(Figure 1)**, with B-6 having a larger particle size.

Yield of NFM

ANMM gave a %yield of 79.4±1.7 to 88.9±1.2, B-5 showed a maximum **(Figure 1)**.

% Drug entrapment

The drug entrapment of ANMM was pragmatic in the range of 74.8±1.52 to 84.5±2.54, Formulation with more NFM (B-7 to B-9) gave good ACR entrapment **(Figure 1)**.

Swelling measurement

By analyzing the ACR release pattern, the ANMM can be used to govern the extent of mucoadhesion. The swelling index shrank steadily as the NFM concentration decreased. Among the batch B-9 samples, batch B-8 and B-9 were the most swollen. NFM may not have been present in adequate masses to cause swelling. B-7, B-8, and B-9 likely contain the highest concentrations of NFM. In NFM, several polar compounds enable it to absorb and hold water, as well as have swelling properties.

In vitro mucoadhesion time

The mucoadhesion of all batches of NFM ranged from 11.2±0.18 (B-1) to 14.2±0.05 (B-9) **(Figure 1)**. With an increase in NFM content aided by methocel 934 P levels, mucoadhesion time was considered to increase.

In vitro drug release

NFM was studied for dissolution. A comparison of formulations B-6 and B-4 shows 91.9±4.5% and 90.8±1.7% **(Figure 2)** of good ACR release at the end of 10 h.

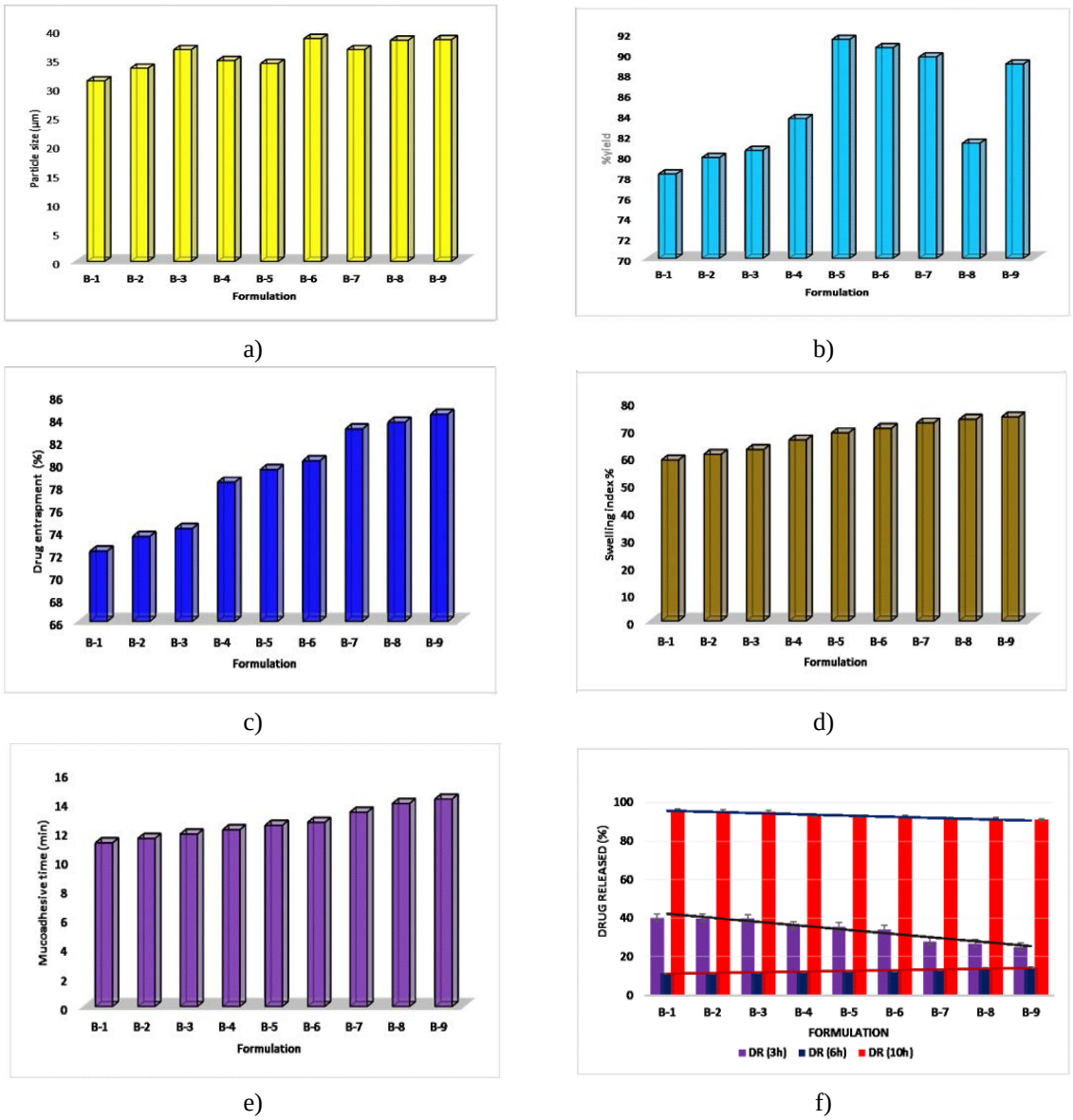

Figure 1. Particle size. % yield, drug entrapment, swelling index, mucoadhesive time and drug release at 3h, 6h, and 10h of microspheres

ACR estimation

With a UV-VIS spectrometer, a calibration curve for ACR was obtained for the estimation in 0.1M HCl solution at 254 nm λ_{max}. Beer's law witnessed that the calibration curve was in the range of 0-10 µg/ml (repeated thrice). Data like this is helpful in determining content uniformity.

Fit summary

In **Table 2**, the fit summary for the responses to DR at 3h, 6h, and 10h is shown.

Table 2. Fit summary for the responses

Source	Sequential p-value	Adjusted R^2	Predicted R^2
Fit summary for the response 1 (DR at 3h)			
Linear	< 0.0001	0.9542	0.9236
2FI	0.3338	0.9553	0.8936
Quadratic	**0.0035**	**0.9983**	**0.9942**
Cubic	0.8156	0.9966	0.9217
Fit summary for the response 2: (DR at 6h)			
Linear	0.0011	0.8625	0.7849
2FI	0.7812	0.8378	0.6120
Quadratic	**< 0.0001**	**0.9999**	**0.9998**
Cubic	1.0000		
Fit summary for the response 3: (DR at 10h)			
Linear	< 0.0001	0.9572	0.9366
2FI	1.0000		
Quadratic	**0.0019**	**0.9987**	**0.9957**
Cubic	0.8660	0.9970	0.9318

ANOVA for Quadratic model

ANOVA for the responses i.e., DR at 3h, 6h, and 10h were denoted in **Table 3**.

Table 3. ANOVA for the responses

Source	Sum of Squares	df	Mean Square	F-value	p-value	
ANOVA for the response 1: DR at 3h (%)						
Model	284.80	5	56.96	927.84	< 0.0001	significant
A-Methpol 934P	4.51	1	4.51	73.41	0.0033	
B-NFM	270.68	1	270.68	4409.29	< 0.0001	
AB	1.82	1	1.82	29.69	0.0121	
A^2	0.1800	1	0.1800	2.93	0.1854	
B^2	7.61	1	7.61	123.88	0.0016	
Residual	0.1842	3	0.0614			
Cor Total	284.98	8				
ANOVA for the response 2: DR at 6h (%)						
Model	51.66	5	10.33	27897.00	< 0.0001	significant
A-Methpol 934P	0.9600	1	0.9600	2592.00	< 0.0001	
B-NFM	45.37	1	45.37	1.225E+05	< 0.0001	
AB	0.0900	1	0.0900	243.00	0.0006	
A^2	0.0089	1	0.0089	24.00	0.0163	
B^2	5.23	1	5.23	14113.50	< 0.0001	

Residual	0.0011	3	0.0004		
Cor Total	51.66	8			
ANOVA for the response 3: DR at10h (%)					
Model	26.73	5	5.35	1202.70	< 0.0001
A-Methpol 934P	0.6667	1	0.6667	150.00	0.0012
B-NFM	25.22	1	25.22	5673.38	< 0.0001
AB	0.0000	1	0.0000	0.0000	1.0000
A^2	0.0000	1	0.0000	0.0000	1.0000
B^2	0.8450	1	0.8450	190.13	0.0008
Residual	0.0133	3	0.0044		
Cor Total	26.74	8			

The model's F-value of 927.84 designates that the model is significant for the response of DR at 3h. There is only a 0.01% chance coincidental that a large F-value would occur as a result of noise. Model terms are significant when P-values are less than 0.05. Model terms A, B, AB, B^2 are significant. Values >0.1 indicate the model is not significant. It may be beneficial to reduce model terms (excluding those required for supporting hierarchy) if there are many insignificant terms in your model.

Furthermore, the response of DR at 6h signposts that the model is significant since its F-value is 27897.00. In this case, A, B, AB, A^2, and B^2 correspond to significant model terms.

In contrast, the model F-value of 1202.70 signposts that the model is significantly based on the response of DR at 10h. In this case, A, B, B^2 are significant model terms.

ANOVA details of DR at various intervals

The ANOVA for DR at 3 h, 6 h, and 10 h is shown in **Table 3**. This model is significantly based on the F-value. In these cases, X_1, X_2, and X_3 were significant terms in the model. Any value > 0.1 signposts that the model is not significant. As a result of these coding factors, the final equation for DR at 3h was as follows: DR at 3h = +35.47-0.8667A-6.72B-0.6750AB-0.3000A2-1.95B2, DR at 6h (%) was as follows: DR at 6h = +69.02-0.4000A-2.75 B+0.1500AB +0.0667A2+1.62B2, the DR at 10h was as follows: DR at 10 as: DR at 10h=+92.87-0.3333A-2.05B+0.0000AB+0.0000A^2+0.6500B^2. For the given levels of each factor, the equation in terms of coded factors can be used to predict the response. Factors with a high level are automatically coded as +1 and those with a low level as -1. By comparing the coefficients of the factors, the coded equation can identify the comparative control of the factors.

Diagnostic analysis for DR at various intervals

Diagnostic plots were used to observe the goodness of fit of the DR at 3h **(Figures 2a-d)**. At the normal prospect line of the plot of outwardly studentized residuals, a maximum of colored points represents the DR at 3h, thereby confirming that the residuals are normal and suggesting a suitable analysis of the response data. There are no significant residuals, suggesting the hypothesis of normality holds **(Figure 2a)**. The DR at 3h was within the limits, as shown by the plot of residuals against predicted values. By looking at the random distribution of studentized residuals, it appears that the assumption of constant variance **(Figure 2b)** is true. Variables predictive of DR at 3h of testing were identified by plotting residuals against run numbers. In **Figure 2c**, all the points indicate that there were no faraway observations during the run. Based on **Figure 2d**, it was observed that the predicted and actual DR values at 3h were very similar. Similar findings were made even at DR after 6 h **(Figures 2e–h)** and 10 h **(Figures 2 i-l)**.

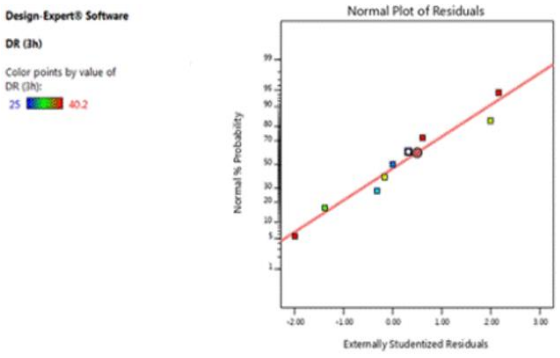
Design-Expert® Software
DR (3h)
Color points by value of DR (3h):
25 40.2
Normal Plot of Residuals
Normal % Probability
Externally Studentized Residuals

a)

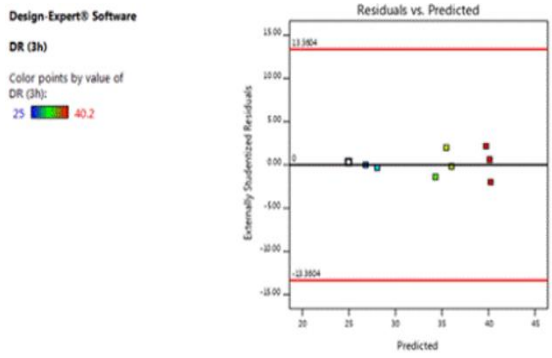
Design-Expert® Software
DR (3h)
Color points by value of DR (3h):
25 40.2
Residuals vs. Predicted
Externally Studentized Residuals
Predicted

b)

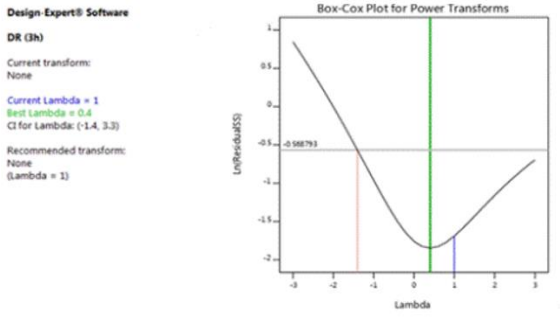
Design-Expert® Software
DR (3h)
Current transform:
None
Current Lambda = 1
Best Lambda = 0.4
CI for Lambda: (-1.4, 3.3)
Recommended transform:
None
(Lambda = 1)
Box-Cox Plot for Power Transforms
Ln(ResidualSS)
Lambda

c)

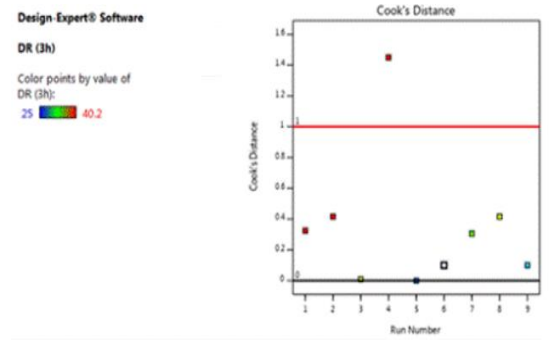
Design-Expert® Software
DR (3h)
Color points by value of DR (3h):
25 40.2
Cook's Distance
Cook's Distance
Run Number

d)

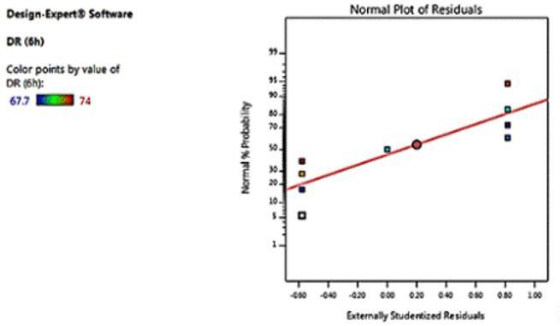
Design-Expert® Software
DR (6h)
Color points by value of DR (6h):
67.7 74
Normal Plot of Residuals
Normal % Probability
Externally Studentized Residuals

e)

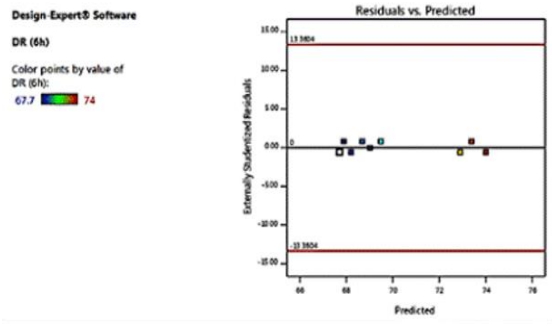
Design-Expert® Software
DR (6h)
Color points by value of DR (6h):
67.7 74
Residuals vs. Predicted
Externally Studentized Residuals
Predicted

f)

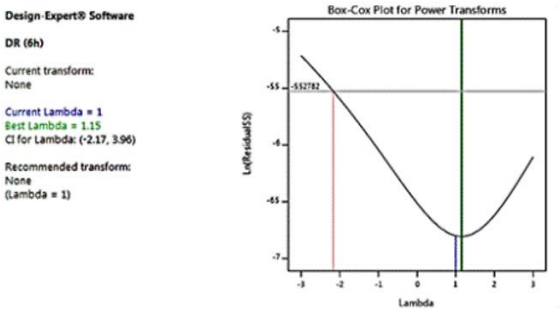
Design-Expert® Software
DR (6h)
Current transform:
None
Current Lambda = 1
Best Lambda = 1.15
CI for Lambda: (-2.17, 3.96)
Recommended transform:
None
(Lambda = 1)
Box-Cox Plot for Power Transforms
Ln(ResidualSS)
Lambda

g)

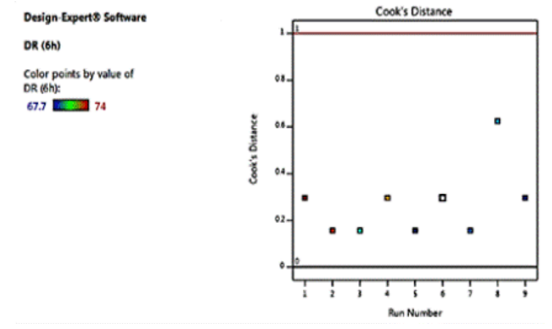
Design-Expert® Software
DR (6h)
Color points by value of DR (6h):
67.7 74
Cook's Distance
Cook's Distance
Run Number

h)

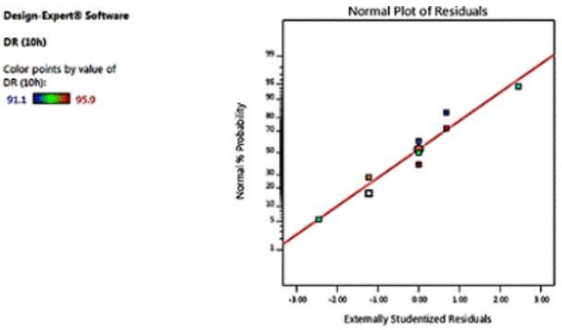
Design-Expert® Software
DR (10h)
Color points by value of DR (10h):
91.1 95.9
Normal Plot of Residuals
Normal % Probability
Externally Studentized Residuals

i)

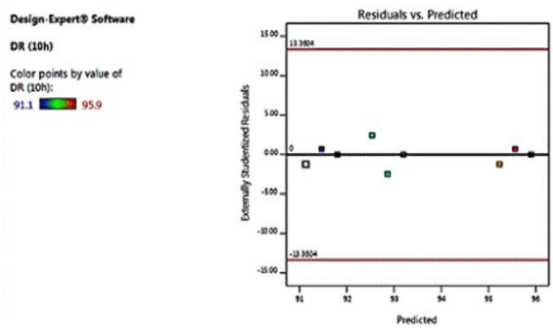
Design-Expert® Software
DR (10h)
Color points by value of DR (10h):
91.1 95.9
Residuals vs. Predicted
Externally Studentized Residuals
Predicted

j)

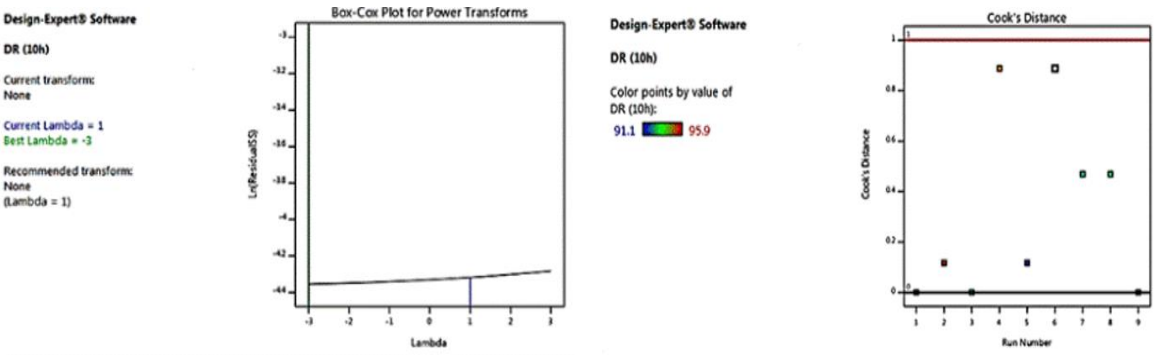

k) l)

Figure 2a-l. Plots showing the interaction effects of polymers on ACR release at 3h (a-d), 6h (e-h), and 10h (i-l) for NFM

Figure 3 is the representation of the DR at 3h, 6h, and 10h with 3D response plots.

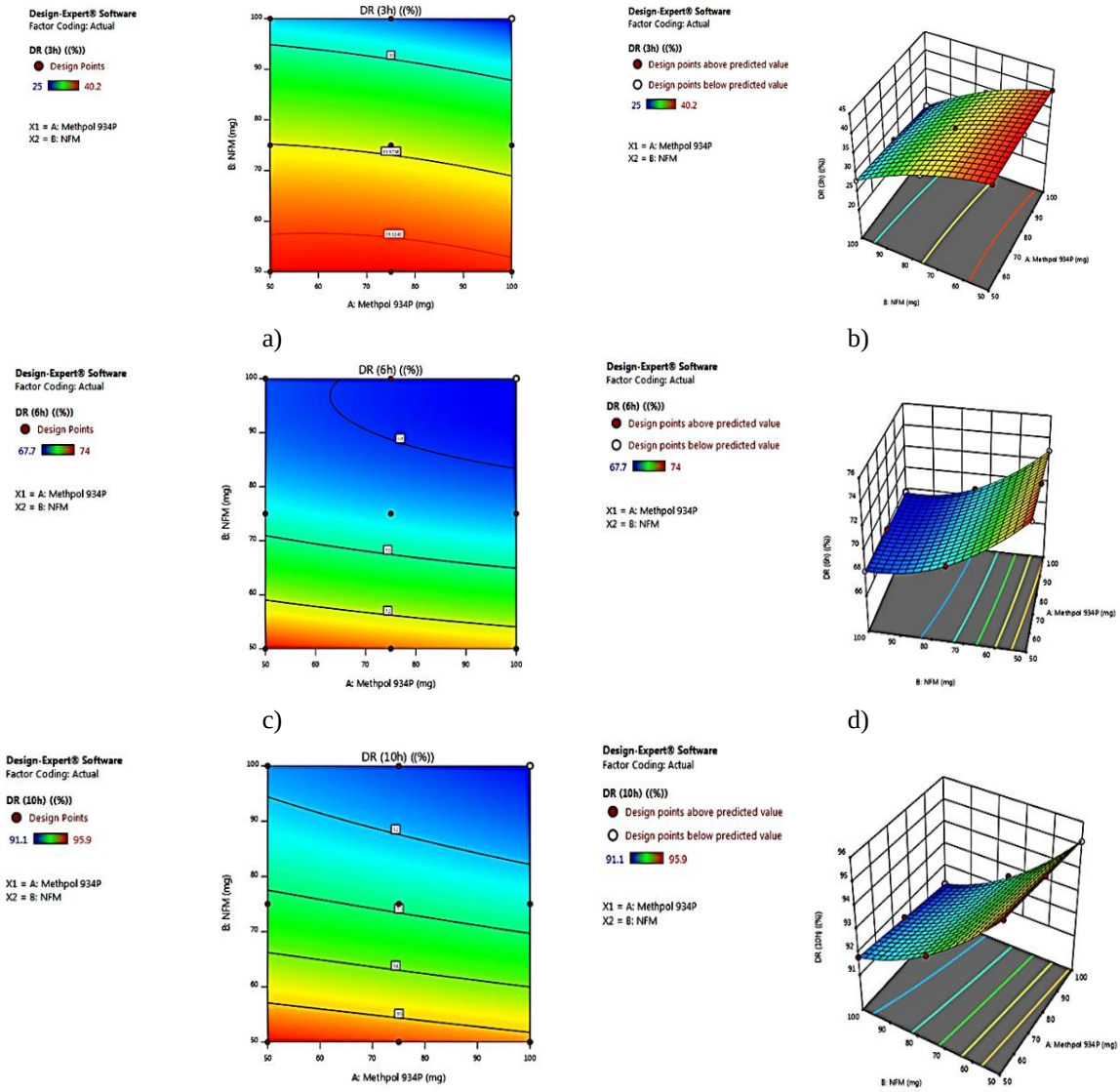

a) b)

c) d)

e) f)

Figure 3. Contour plot and 3D response plots for DR at 3h, 6h, and 10h

Plots like this show the sway of same time two-factor response. The contour and response surface plots respectively **(Figure 3)** show that a corresponding increase in the mucoadhesion time of the formulation.

CONCLUSION

When the microspheres are digested, the Acyclovir (ACR) is released into the stomach. ACVR's formulation included Neem (*Azadirachta indica*) fruit mucilage (NFM) combined with Methocel 934 P. The mucoadhesive polymers control the amount and rate of Acyclovir (ACR) release in the mucoadhesive drug delivery system. Compared to other formulations. The quantities of NFM are less in formulations B-1 to B-3, indicating good entrapment of ACR. NFM content in all batches increased with an increase in mucoadhesive time. It can be concluded from this study that mucoadhesive microspheres of ACR with NFM aided by methocel 934 P meet the ideal requirement for mucoadhesive microspheres, which can enhance retention and availability in the stomach for efficient and intended drug delivery.

ACKNOWLEDGMENTS : None

CONFLICT OF INTEREST : None

FINANCIAL SUPPORT : None

ETHICS STATEMENT : None

REFERENCES

1. Patel D, Sawant KK. Oral bioavailability enhancement of acyclovir by self-microemulsifying drug delivery systems (SMEDDS). Drug Dev Ind Pharm. 2007;33(12):1318-26.
2. Wang M, Hou J, Yu DG, Li S, Zhu J, Chen Z. Electrospun tri-layer nanodepots for sustained release of acyclovir. J Alloys Compd. 2020;846:156471.
3. Fletcher C, Bean B, McLeod DC. Evaluation of oral acyclovir therapy. Drug Intell Clin Pharm. 1985;19(7-8):518-24.
4. Uchegbu M, Okoli I, Esonu B, Iloeje M. The grovving importance of neem (Azadirachta indica A. Juss) in agriculture, industry, medicine and Eenvironment: A review. Res J Med Plant. 2011;5(3):230-45.
5. Uzzaman S. Pharmacological activities of neem (Azadirachta indica): A review. Int J Pharmacogn Life Sci. 2020;1:38-41.
6. Hindustan AA, Babu UA, Nagesh K, Kiran DS, Madhavi KB. Fabrication of glimepiride Datura stramonium leaves mucilage and poly vinyl pyrrolidone sustained release matrix tablets: in vitro evaluation. Kathmandu Univ J Sci, Eng Technol. 2012;8(1):63-72.
7. Shravani Y, Ahad HA, Haranath C, Gari Poojitha B, Rahamathulla S, Rupasree A. Past Decade Work Done On Cubosomes Using Factorial Design: A Fast Track Information for Researchers. Int J Life Sci Pharma Res. 2021;11:124-35.
8. Ahad HA, Kumar CS, Ravindra BV, Sasidhar CG, Ramakrishna G, Venkatnath L, et al. Characterization and permeation studies of Diltiazem hydrochloride-ficus reticuleta fruit mucilage Transdermal patches. Int J Pharm Sci Rev Res. 2010;1(2):32-7.
9. Ahad HA, Haranath C, Varam NJ, Ksheerasagare T, Krishna JV, Teja ST. Liver shielding activity of Ficus benghalensis fruit extracts contrary to perchloromethane prompted toxic hepatitis in New Zealand albino rats. Res J Pharm Technol. 2021;14(7):3739-43.
10. Ahad HA, Haranath C, Rahul Raghav D, Gowthami M, Naga Jyothi V, Sravanthi P. Overview on Recent Optimization Techniques in Gastro Retentive Microcapsules by Factorial Design. Int J Pharm Sci Res. 2019;10(9):247-54.
11. Dil EA, Ghaedi M, Asfaram A. Application of hydrophobic deep eutectic solvent as the carrier for ferrofluid: a novel strategy for pre-concentration and determination of mefenamic acid in human urine samples by high performance liquid chromatography under experimental design optimization. Talanta. 2019;202:526-30.
12. Hindustan AA, Sreeramulu J, Narasimha RD, Guru PP, Ramyasree P. Fabrication and In vitro Evaluation of High density Gastro retentive Microspheres of Famotidine with Synthetic and Natural Polymers. Indian J Pharm Educ Res. 2012;46(1):48.
13. Karabulut I, Turan S, Ergin G. Effects of chemical interesterification on solid fat content and slip melting point of fat/oil blends. Eur Food Res Technol. 2004;218(3):224-9.

14. Raina H, Kaur S, Jindal AB. Development of efavirenz loaded solid lipid nanoparticles: Risk assessment, quality-by-design (QbD) based optimisation and physicochemical characterisation. J Drug Deliv Sci Technol. 2017;39:180-91.
15. Yadav S, Padhi S, Kumar P. Design and characterization of floating tablet of ondansetron hydrochloride for gastricretation. Pharmacophore. 2014;5(4):467-76.
16. Patel HR, Patel RR, Patel L, Patel Y, Raval A. Preparation and in vitro characterization of non effervescent floating delivery system of cefpodoxime proxetil. Pharmacophore. 2016;7(2):132-40.
17. Annepogu H, Hindustan Abdul AH, Nayakanti D. Determining the best poloxamer carrier for thiocolchicoside solid dispersions. Turk J Pharm Sci. 2020;17(4):372.
18. Madane MA, Shinde AD. Formulation and evaluation of microsponge based drug delivery system of levonorgestrel. Pharmacophore. 2016;7(4).
19. Ahmed OA, Hosny KM, Al-Sawahli MM, Fahmy UA. Optimization of caseinate-coated simvastatin-zein nanoparticles: improved bioavailability and modified release characteristics. Drug Des Devel Ther. 2015;9:655.
20. Chinthaginjala H, Abdul H, Reddy APG, Kodi K, Manchikanti SP, Pasam D. Nanosuspension as Promising and Potential Drug Delivery: A Review. Int J Life Sci Pharma Res. 2020;11:59-66.
21. Kaur G, Chandel P, Harikumar S. Formulation development of self nanoemulsifying drug delivery system (SNEDDS) of celecoxib for improvement of oral bioavailability. Pharmacophore. 2013;4(4):120-33.
22. Hiremath J, Kang KI, Xia M, Elaish M, Binjawadagi B, Ouyang K, et al. Entrapment of H1N1 influenza virus derived conserved peptides in PLGA nanoparticles enhances T cell response and vaccine efficacy in pigs. PLoS One. 2016;11(4):e0151922.
23. Frias I, Neves AR, Pinheiro M, Reis S. Design, development, and characterization of lipid nanocarriers-based epigallocatechin gallate delivery system for preventive and therapeutic supplementation. Drug Des Devel Ther. 2016;10:3519.
24. Patel JK, Patel RP, Amin AF, Patel MM. Formulation and evaluation of mucoadhesive glipizide microspheres. AAps Pharm Sci Tech. 2005;6(1):E49-55.
25. Tao Y, Lu Y, Sun Y, Gu B, Lu W, Pan J. Development of mucoadhesive microspheres of acyclovir with enhanced bioavailability. Int J Pharm. 2009;378(1-2):30-6.
26. Dhyani A, Kumar G. A New Vision to Eye: Novel Ocular Drug Delivery System. Pharmacophore. 2019;10(1):13-20.
27. Harsha SN, Aldhubiab BE, Nair AB, Alhaider IA, Attimarad M, Venugopala KN, et al. Nanoparticle formulation by Büchi B-90 Nano Spray Dryer for oral mucoadhesion. Drug Des Devel Ther. 2015;9:273.
28. Md S, Ahuja A, Khar RK, Baboota S, Chuttani K, Mishra AK, et al. Gastroretentive drug delivery system of acyclovir-loaded alginate mucoadhesive microspheres: formulation and evaluation. Drug Deliv. 2011;18(4):255-64.
29. Goldberg DE, Scheiner SM. ANOVA and ANCOVA: field competition experiments. Des Anal Ecol Exp. 2001;2:69-93.